ORIGINAL RESEARCH

Effect of biochar type on infiltration, water retention and desiccation crack potential of a silty sand

Rojimul Hussain[1] · Sanandam Bordoloi[1] · Piyush gupta[1] · Ankit Garg[2] · K. Ravi[1] · S. Sreedeep[1] · Lingaraj Sahoo[3]

Abstract

Biochar is a carbon-rich material obtained after thermochemical conversion of biomass under no oxygen environment. The effect of biochar amendment on soil properties, such as water retention, infiltration and desiccation crack potential was studied in the recent years. However, the effect of biochar or feedstock type on these properties is not explicit. This study investigates the effect of two different (in terms of feedstock) types of biochar on the water retention, infiltration and desiccation cracking behavior of compacted silty sand. Water retention characteristics, infiltration rate and the progression of desiccation cracks were measured after compacting soil amended with 5–10% (w/w) biochar produced from water hyacinth (WHB) and mesquite. Measurements were also taken for an unpyrolyzed material coir pith (CP, sourced from coconut husk)-amended soil for comparing the results of biochar-amended soil. The results show that the amendment of 5% to 10% biochar increased the maximum water holding capacity (θ_s), air entry value (AEV) and water content at 1500 kPa (θ_{1500}) of the soil, whereas decreased the infiltration rate and peak crack intensity factor (CIF) of the soil. Moreover, the application of CP increased the infiltration rate. The amendment of WHB showed the highest increment in AEV and θ_{1500} and the highest decrement in infiltration rate and CIF compared to the other amendments. Based on the results, it is advisable to use the WHB-amended soil in bioengineered structures that could promote the growth of vegetation by higher water retention and could reduce the potential of leachate formation by decreasing water infiltration and desiccation crack potential.

✉ K. Ravi
ravi.civil@iitg.ac.in

Rojimul Hussain
rojmul.hussain@iitg.ac.in

Sanandam Bordoloi
sanandam@iitg.ac.in

Piyush gupta
iitbiitgiitk@gmail.com

Ankit Garg
ankit@stu.edu.cn

S. Sreedeep
srees@iitg.ac.in

Lingaraj Sahoo
ls@iitg.ac.in

1 Department of Civil Engineering, Indian Institute of Technology Guwahati, Guwahati, India

2 Department of Civil and Environmental Engineering, Shantou University, Shantou, China

3 Department of Biosciences and Bioengineering, Indian Institute of Technology Guwahati, Guwahati, India

1 Introduction

The amendment of biochar in soil gained momentum in geotechnical and geoenvironmental engineering, e.g., landfill cover and other bioengineered structure, due to its multiple beneficial features, such as carbon sequestration (Van Zwieten et al. 2010), removal of methane gas from landfill cover soil (Reddy et al. 2014; Wong et al. 2016), improvement of vegetation growth (Cao et al. 2014; Chen et al. 2016) and removal of organic and inorganic pollutant, especially heavy metals from soil in mining sites (Fellet et al. 2011; Yargicoglu and Reddy 2017). Biochar is a solid product obtained after pyrolysis or gasification of biomass under the absence or limited content of oxygen in a closed container (Lehmann and Joseph 2015). It is characterized by high porosity, large specific surface area (SSA), high pH value, presence of surface functional group (carboxyl, hydroxyl and phenolic) and high nutrient content that could influence the physicochemical and hydraulic properties of soil (Ahmad et al. 2014; Reddy et al. 2015; Tan et al. 2015; Yang et al. 2017).

Previous studies reported that the amendment of biochar in soil increased the Atterberg limits and the optimum moisture content (OMC) and decreased the maximum dry density (MDD) (Yaghoubi and Reddy 2011; Ni et al. 2018; Williams et al. 2018). It was also found that the saturated hydraulic conductivity decreased in sandy soil while increased in clayey soil when biochar was amended (Uzoma et al. 2011; Igalavithana et al. 2017; Wong et al. 2018).

The amendment of biochar in soil could alter the soil water retention characteristics (SWRC), infiltration rate and desiccation crack potential of soil (Downie et al. 2009; Ibrahim et al. 2013; Zong et al. 2014; Wong et al. 2017). This is conceptually highlighted in Fig. 1 where it is hypothesized that the amendment of biochar having intra-pores (pores within biochar), which would change the pore size distribution of the soil and hence the water retention, infiltration rate and desiccation crack. These have been extensively studied for loose soil suitable for agriculture (Major et al. 2012; Ouyang et al. 2013; de-Melo-Carvalho et al. 2014; Prober et al. 2014; Moragues-Saitua et al. 2017; Chen et al. 2019). However, limited studies are available for soil in geotechnical and geoenvironmental engineering structures, e.g., landfill cover (Wong et al. 2017), bioengineered slopes and embankment (Bordoloi et al. 2018b; Ni et al. 2018) where soils often compacted, have higher design life and generate higher suction due to drying (Wall and Zeiss 1995; Harshani et al. 2015). Wong et al. (2017) reported an increased water retention of kaolin clay after amendment of peanut shell biochar. Recently, Bordoloi et al. (2018b) investigated the water retention and desiccation potential of sand amended with biochar derived from water hyacinth by measuring suction ranges from near saturation to wilting point. It was reported an increased water retention and decreased crack potential quantified by a crack intensity factor (CIF, defined as the ratio of total crack area to the total soil surface area considered).

Cracks form in soil when the tensile stress developed in soil due to the generation of suction exceeds the tensile strength of the soil (Corte and Higashi 1964). The presence of cracks in landfill cover soil could lead to the emission of methane gas to the atmosphere, increase the formation of leachate by enhancing the infiltration rate during rainfall and increase the potential of erosion, whereas in agricultural soil it could lead to a rapid flow of nutrient causing a loss of nutrient (Coles and Trudgill 1985; Albright et al. 2006; Indraratna et al. 2008; Costa et al. 2013). The infiltration rate is an important parameter for engineered structures where a higher infiltration rate could lead to a generation of leachate and pore water pressure, which are against the integrity of these structures. The amendment of biochar in agricultural soil decreased the infiltration rate, which was measured using a mini-disk infiltrometer (Ibrahim et al. 2013; Githinji 2014).
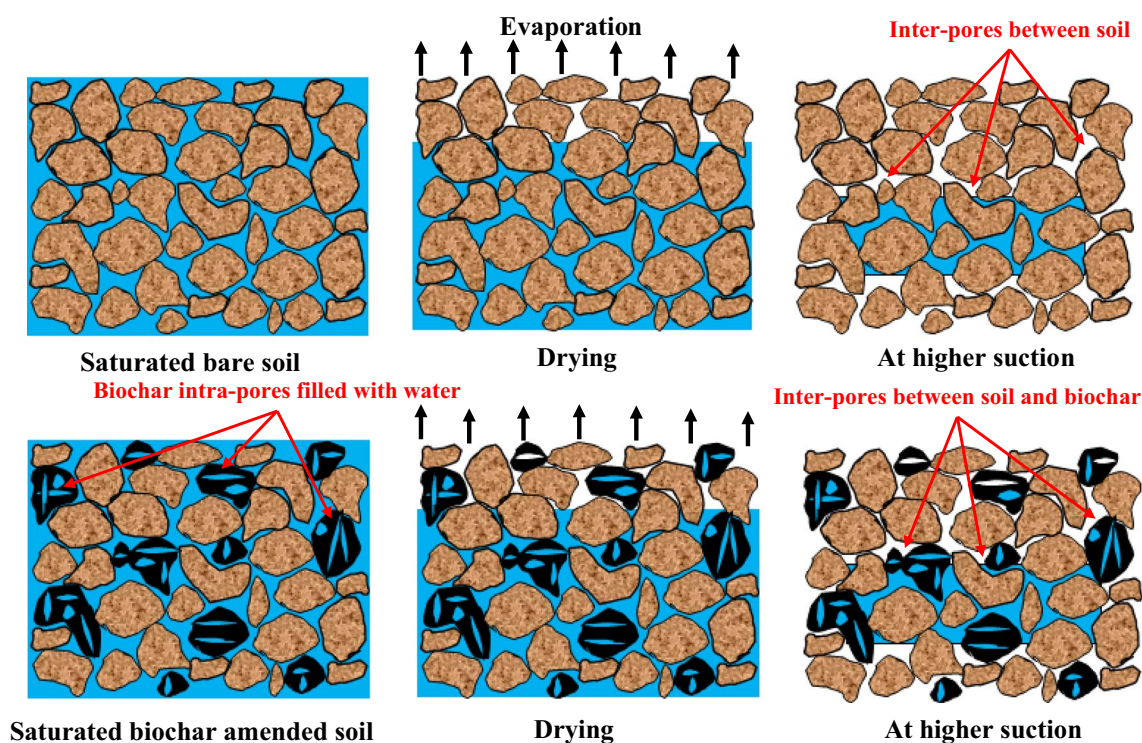

Fig. 1 Conceptual diagram showing saturated to drying state of the bare and biochar-amended soil

Even though the previous studies investigated the water retention, infiltration rate and desiccation potential of biochar amended soil, the effect of biochar type on these properties was not considered. Any alteration in these properties of soil amendment with biochar could be mainly due to the distinct characteristics of the biochar, including intra-pores, surface functional group, cation exchange capacity, etc., which are highly dependent on the type of feedstock or biochar (Lei and Zhang 2013; Suliman et al. 2017; Wu et al. 2019). Biochar of different feedstock type could be hydrophilic or hydrophobic depending on the type of functional group and could have different porosities that would definitely influence the water retention and infiltration rate of soil after amendment (Jeffery et al. 2015; Hussain et al. 2020a, 2020b). Thus, studies are needed to consider the effect of biochar type on the water retention, infiltration rate and desiccation potential of soil. The objective of the present study is to investigate the effect of biochar type on the water retention, infiltration and desiccation crack potential of compacted silty sand. Soil columns were prepared by compacting soil amended with 5–10% (w/w) biochar produced from feedstock of water hyacinth (WHB) and mesquite wood (CB) at 500 °C for monitoring matric suction, volumetric water content, infiltration rate and desiccation crack. Similarly, soil columns were also prepared for coir pith (CP, an un-pyrolyzed material)-amended soil for comparing the results of biochar-amended soil.

2 Materials and method

2.1 Soil

Soil for the study was collected from a hillside located inside the campus of Indian Institute of Technology (IIT) Guwahati in North-eastern province of India (26.19°N, 91.69°E). Dead roots, stones and any other impurity in the soil were manually removed. Thereafter the soil was characterized for basic and index properties based on the referral provided by ASTM standards (ASTM C128–15 (2015); ASTM D422–63 (2007); ASTM D698–12 (2012); ASTM D854 (2010); ASTM D4318–10 (2010); ASTM D4972 (2018)). The properties of the soil are reported in Table 1.

2.2 Biochar

Two different types of biochar (based on different types of feedstock) and a coir pith (CP) were used in this study. The first biochar was made in the laboratory from water hyacinth (*Echhornia crassipes,* an aquatic plant) as feedstock. The water hyacinth (WH) plants as feedstock were collected from Deepor Beel lake in Assam, northeast India (26.13°N, 91.66°E). All the required WH plants were collected from the same water body to minimize any genetic variation. The collected WH plants were dried in air and cut into smaller (20–40 mm) pieces. Pyrolysis of the dried WH plants was carried out at 500 °C for a period of 45 min. The second biochar was commercial biochar (CB) obtained from Greenfield Eco. Pvt. Ltd., and produced from the hardwood of mesquite

Table 1 Basic and index properties of the soil tested

Soil property	Value	ASTM
Specific gravity	2.68 ± 0.04	ASTM D854 (2010)
pH	4.5 ± 0.07	ASTM D4972 (2018)
Water absorption capacity (%)	35.6 ± 1.41	ASTM C128–15 (2015)
Particle size distribution (%)		ASTM D422–63 (2007)
Coarse sand (4.75 mm-2 mm)	6	
Medium sand (2 mm-0.425 mm)	20	
Fine sand (0.425 mm-0.075 mm)	25	
Silt (0.075 mm-0.002 mm)	29	
Clay (< 0.002 mm)	20	
Atterberg limits (%)		ASTM D4318–10 (2010)
Liquid limit	37	
Plastic limit	26	
Shrinkage limit	15	
Compaction properties		ASTM D698–12 (2012)
Optimum moisture content (%)	17	
Maximum dry density (kg/m^3)	1700	
Classification (USCS)	Silty sand (SM)	ASTM D2487–11 (2011)

Value in the table represents the average value ± standard deviation

(*Prosopis juliflora*) as feedstock at 500 °C and 45 min residence time. WH and mesquite are two fast-growing invasive weeds causing many problems to the environment; thus, production of biochar could at least minimize the problem (Malik et al. 2007; Angalaeeswari and Kamaludeen 2017). The CP used in this study was a dried unpyrolyzed material sourced from coconut husk. The coarse WH biochar (WHB) and CB obtained after pyrolysis were crushed using a mechanical crusher, and thereafter, all the biochar and CP were sieved through 2 mm sieve for minimizing the influence of particles size. The images of the biochar and CP are highlighted in Fig. 2a–d. The elemental composition of the biochar was determined using combustion technique as per the procedure described in Bird et al. (2017). The ash content and cation exchange capacity were measured by the ammonium acetate method (Thomas 1982) and the method described in ASTM E1755-01 (2007). The contact angle of wetting was measured by following the sessile drop method as described in Jeffery et al. (2015). The surface functional groups present in the biochar and CP were determined by the Fourier transform infrared spectroscopy (FTIR) test using a Fourier transform infrared spectrophotometer (IRAffinity-1, Shimadzu, Japan). To observe the surface morphology, field emission scanning electron microscopy (FESEM) images were captured using a Sigma-300 (Zeiss) variable pressure field emission scanning electron microscope operated with 2–10 kV accelerating voltage. Images were captured at different magnifications ranging from 50 × to 40K ×. The properties of biochars and CP are presented in Table 2.

2.3 Test procedure

2.3.1 Preparation of soil column

The test setup used for the experimental study is presented in Fig. 3. PVC mold of size 250 mm diameter and 250 mm length with a perforated base allowing water drainage were fabricated for preparing compacted soil column. Holes were drilled in the diagonal direction of the mold at a depth of 120 mm for accommodating suction and moisture content sensors. For biochar-amended soil, the soil and biochar at 5–10% (w/w) were dry mixed in an aluminum pan. Thereafter, water corresponding to 90% of the maximum dry density (0.9MDD) obtained from the standard Proctor test (compaction curve) was added, mixed uniformly and incubated for a period of 24 h by sealing inside a desiccator for moisture equilibration. The mixture was then statically compacted at a dry density equal to 0.9MDD in three layers up to a height of 170 mm from the base of the mold. The selection of compaction density of 0.9MDD and the corresponding water content was based on the compaction criteria adopted for many geotechnical and geoenvironmental structures reported in the
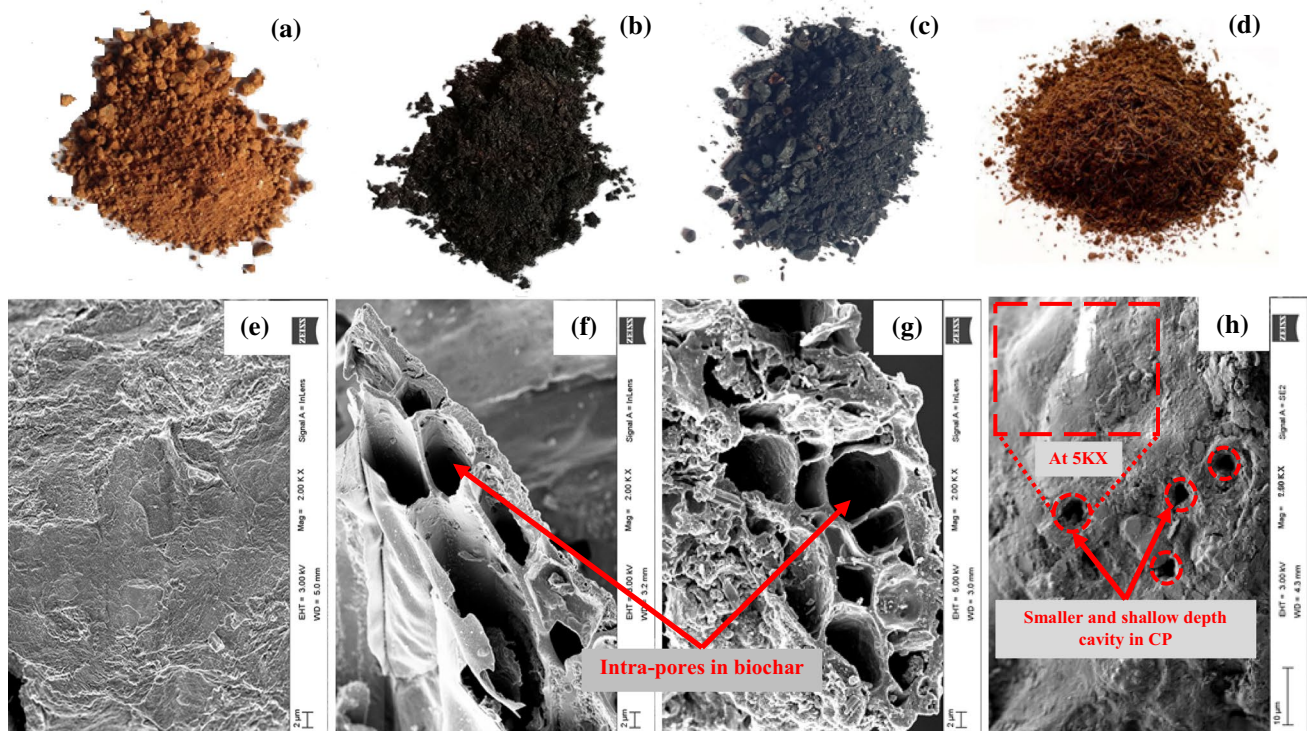

Fig. 2 Raw images of **a** bare soil, **b** water hyacinth biochar (WHB), **c** commercial biochar (CB) and **d** coir pith (CP) and FE-SEM images (at 2K ×) of **e** bare soil, **f** WHB, **g** CB and **h** CP

Table 2 Properties of the selected biochars and coir pith

	WHB	CB	CP	ASTM/method
Feedstock	Water hyacinth stem sourced from Deepor lake, India	Hardwood of mesquite (*Prosopis juliflora*) by Greenfield Eco. Pvt. Ltd	Coconut husk	–
Pyrolysis process	Slow pyrolysis	Slow pyrolysis	–	–
Pyrolysis temperature (°C)	500	500	–	–
Elemental composition (%)				Combustion technique (Bird et al. 2017)
Carbon (C)	55	71.5	33.64	
Oxygen (O)	44	–	–	
Hydrogen (H)	2	–	–	
Nitrogen (N)	1.88	0.19	2.25	
Phosphorus (P)	–	0.2	0.02	
Potassium (K)	–	2.6	0.05	
Molar ratios				–
H:C	0.05	–	–	
C:N	29	382	15	
Ash content (%)	40	1.9	–	ASTM E1755–01 (2007)
CEC (cmol kg^{-1})	21	18	–	ASTM D7503
Specific gravity	1.2 ± 0.1	1.05 ± 0.1	–	ASTM D854 (2010)
pH	7.7 ± 0.1	8.4 ± 0.22	7.02 ± 0.16	ASTM D4972 (2018)
Water absorption capacity (%)	54.7 ± 0.99	205 ± 12.73	–	ASTM C128–15 (2015)
Average pore size (nm)	35 ± 5	60 ± 4	–	BET analysis
Contact angle of wetting (°)	0	65 ± 3	–	Sessile drop method
EC (dSm^{-1})	–	1.5	0.005	–
Particle size distribution (%)				
Coarse sand (4.75-2 mm)	0	0	–	ASTM D422–63 (2007)
Medium sand (2–0.425 mm)	0	67	–	
Fine sand (0.425–0.075 mm)	30	23	–	
Fine content (< 0.075 mm, silt and clay)	70	10	–	

WHB water hyacinth biochar, *CB* commercial biochar, *CP* coir pith, *CEC* cation exchange capacity, *EC* electric conductivity

literature (Goldsmith et al. 2001; Li et al. 2016). Moreover, the selection of amendment rate of 5–10% was based on the preliminary investigations conducted for the biochars considered in this study.

2.3.2 Measurement of suction, moisture content and soil water retention curve (SWRC)

The matric suction (ψ_m) was measured using MPS-6 sensors, while the volumetric water content (θ) was measured using EC-5 volumetric water content sensors (Decagon devices 2016). The MPS-6 sensors can measure the matric suction in the range of 9–10^5 kPa with an error of ± 10%, and the EC-5 sensors can measure the volumetric water content in the range of 0–100% with an error of ± 3%. These sensors were inserted to the compacted soil/soil-biochar mixture through the predrilled holes at 40 mm from the surface of the compacted soil, as mentioned in the previous section. However, before installation, soil specific calibration for all

the sensors was performed for minimizing any variation or error in reading. The choice of 40 mm sensor depth was based on the influence zone of the moisture sensors (approx. 25 mm either side). For preventing any leakage of water, the open space surrounding the sensor body was sealed using a plastic sealant (Anabond glue). Three replicates for bare soil and three replicates for each 5–10% biochar and CP amended soil were tested.

All the compacted soil columns were placed in a greenhouse (Fig. 3) maintained at a relative humidity of 55 ± 5% and temperature of 25 ± 1 °C. For measuring the soil water retention characteristics or curve (SWRC), all the compacted soil columns were irrigated using a controlled head mariotte bottle until the suction read by the MPS-6 sensor reached a minimum value of around 9 kPa (minimum range of the sensor) or near saturation. Thereafter, it was subjected to a continuous drying until the suction reached a nearly constant peak value. The MPS-6 and the EC-5 sensors were connected to an EM-50 data logger for continuous monitoring
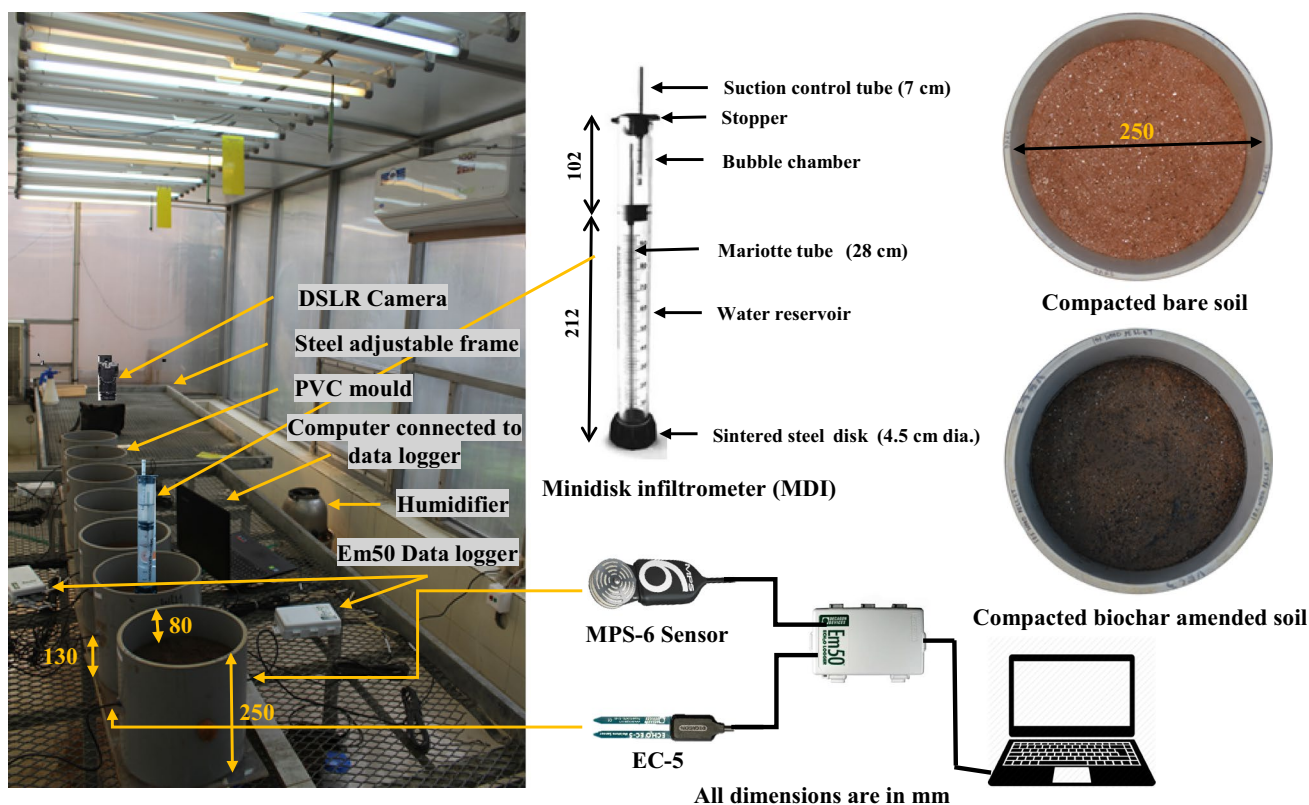
Fig. 3 Experimental setup adopted for the study inside a green house

of suction and moisture content at an interval of 15 min. The suction and volumetric water content data recorded by the data logger were fitted using van Genuchten (1980) model in RETC software (van Genuchten et al. 1991). The air entry value (AEV) was calculated by graphical method (Fredlund et al. 2012), where tangents were drawn along the SWRC curve and the point of crossing of the tangents or the transition point is referred as AEV.

2.3.3 Measurement of infiltration rate

The infiltration test was conducted using a mini-disk infiltrometer (MDI) on the same compacted soil column used for the SWRC measurement (Fig. 3). The selection of MDI for measuring infiltration was likely due to its simplicity to use in laboratory, and there is no need of auguring or disturbing the sample. To start the measurement, the bubble chamber and the reservoir of the MDI were filled with water and a suction head of 2 cm was applied through the suction control tube. The application of the suction head was basically to minimize any flow of water through macro-pores. However, it is to be noted that in the present study, soils are highly compacted where a negligible effect of macro-pores are expected. Similar suction head of 2 cm for measuring infiltration rate using MDI is also found to be adopted by

the previous researchers (Fodor et al. 2011; Bordoloi et al. 2017b). The water-filled MDI was placed vertically straight on the compacted soil surface (Fig. 3) for ensuring proper contact between the sintered disk and the soil surface. The responses of the cumulative volume of water infiltrate (V) with time (t) were recorded at an interval of 60 s. The obtained V-t responses were fitted with a second-degree polynomial equation, and the corresponding fitting parameters were noted. The polynomial equation was further differentiated with respect to time (t) to obtain dV/dt for calculating infiltration rate, I(t) as shown in Eq. 1 below.

$$I(t) = \frac{1}{A}\frac{dV}{dt} \tag{1}$$

where, (dV) is the change of volume of water infiltrated within a given time (dt), and A is the cross-sectional area of the infiltrometer.

2.3.4 Quantification of cracks

In the present study, the surface cracks developed during the drying phase of the samples were quantified by CIF (crack intensity factor). For this, images of the compacted soil surface were captured daily using a commercial DSLR camera (Canon EOS 600D with lens range 18–55 mm and

resolution of 72 dpi) mounted on an adjustable steel frame as shown in Fig. 3. Images were captured from the same height for minimizing any variation in pixel count or area of the images. The captured images were analyzed for cracks using an open-access image processing software Imagej (Rasband 2011) as per the procedure described in Gadi et al. (2017) and Bordoloi et al. (2018a). Figure 4 shows the stepwise procedure adopted for analyzing the image for crack quantification. Digital images captured by the camera were imported into the Imagej software and then cropped for removing the boundary shrinkage. The area (in pixel) of the cropped image was measured and taken as the total soil surface area. In the next step, the cropped images were adjusted to color threshold using RGB color space and the corresponding area of cracks was measured. Thereafter, the CIF was calculated as the ratio of cracks area (A_C) to the total soil surface area (A_T), i.e.

$$CIF(\%) = \frac{A_C}{A_T} \times 100 \tag{2}$$

2.3.5 Statistical analyses

The two-way analysis of variance (ANOVA) was used to determine whether there were any significant differences between the means of the CIF and SWCC parameters with respect to the different biochar amendment rates and the biochar types. The means were compared by post hoc tests such as Tukey and Fisher LSD. The difference is considered statistically significant when the observed p value was less than 0.05 (preset, 95% significance level). The analysis was carried out in Origin Pro (Origin 9) software.

3 Results and discussion

3.1 Properties of the soil and biochar

The FESEM images obtained for the soil, biochars and CP are presented in Fig. 2e–h. The presence of intra-pores in biochar is clearly visible from Fig. 2f–g, whereas the CP has some shallow depth cavity. The functional groups present in the biochar and CP are highlighted in Fig. 5. The presence of water absorptive OH, COOH and C-O functional groups in WHB (Fig. 5) makes it highly hydrophilic compared to the CB where C=C (Alkenes) functional group leads to a slight decrease in hydrophilicity. This higher hydrophilicity of WHB compared to the CB is also evident from the measured contact angle (Table 2). Thus, the variations in physicochemical properties of the produced biochars due to the difference in feedstock type could be easily observed from Table 2, Fig. 2 and Fig. 5, and these, in turn, could lead
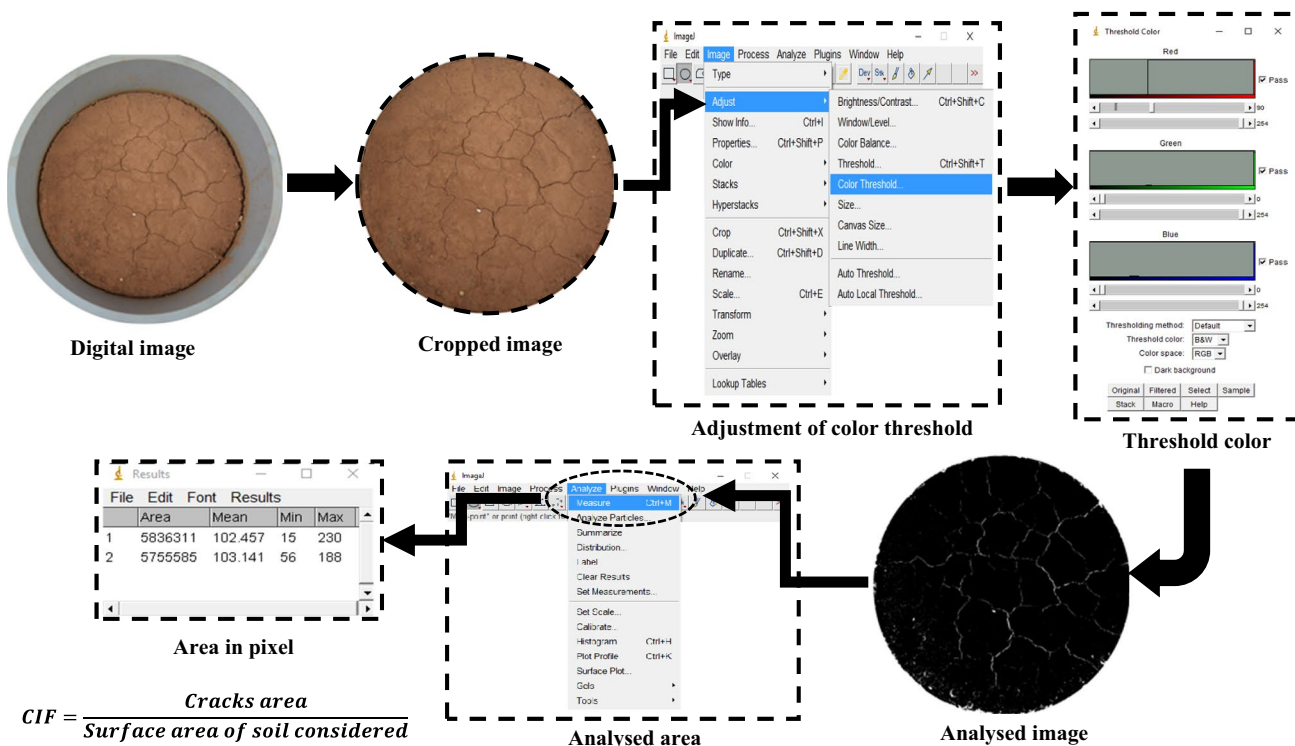

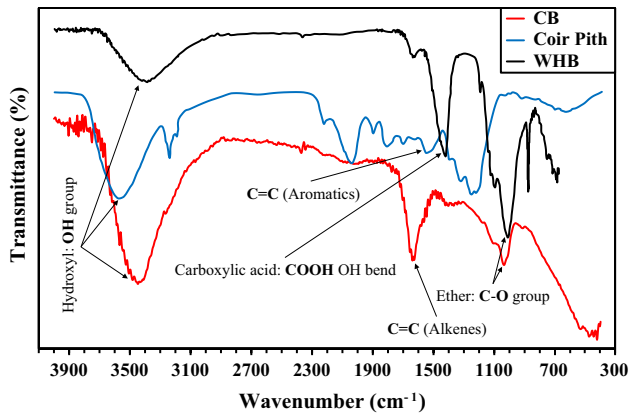**Fig. 4** Process of measuring crack (CIF) using the color threshold technique in ImageJ

Fig. 5 FTIR spectra of the WHB, CB and CP

to the difference in effect of the biochar on soil properties after amendment.

3.2 Effect of biochar on SWRC

Figure 6a–c highlights the SWRCs of the bare soil and soil amended with 5–10%, (w/w) WHB, CB and CP, respectively. The fitting parameters of the SWRCs are presented

in Table 3. The effect of biochar on these fitting parameters, such as, saturated water content or maximum water holding capacity (θ_s), air entry value (AEV), slope (n) and residual water content (θ_r) that defines the water retention characteristics of the soil, is discussed next. The bare soil showed a θ_s of 23%, and it was observed to increase ($p = 0.02 < 0.05$) with the increase in amendment rate of biochar from 5% to 10%. This could be attributed to the higher water absorption capacity of the biochars (Table 2) compared to the soil (Table 1). The higher porosity or large SSA due to the intra-pores present in biochar skeleton (Fig. 2f and g) along with the surface functional groups or bonds especially OH⁻ group (Fig. 4) allow higher water storage or absorption in biochar compared to the soil. The biochar with higher porosity and absorption capacity increased the total porosity and hence θ_s in the biochar-amended soil compared to the bare soil. Among the type of amendment, CP-amended soil showed the highest ($p = 0.1 > 0.05$) θ_s (28.5% and 26% for 10% and 5% biochar, respectively), whereas WHB exhibited the lowest (25% and 24%) (Table 3). The highest θ_s in CP amended soil was attributed to the higher total porosity due to the formation of inter-pores or preferential path between the interface of soil particle and the CP (Bordoloi et al. 2017a). The total porosity comprises of inter-porosity by inter-pores
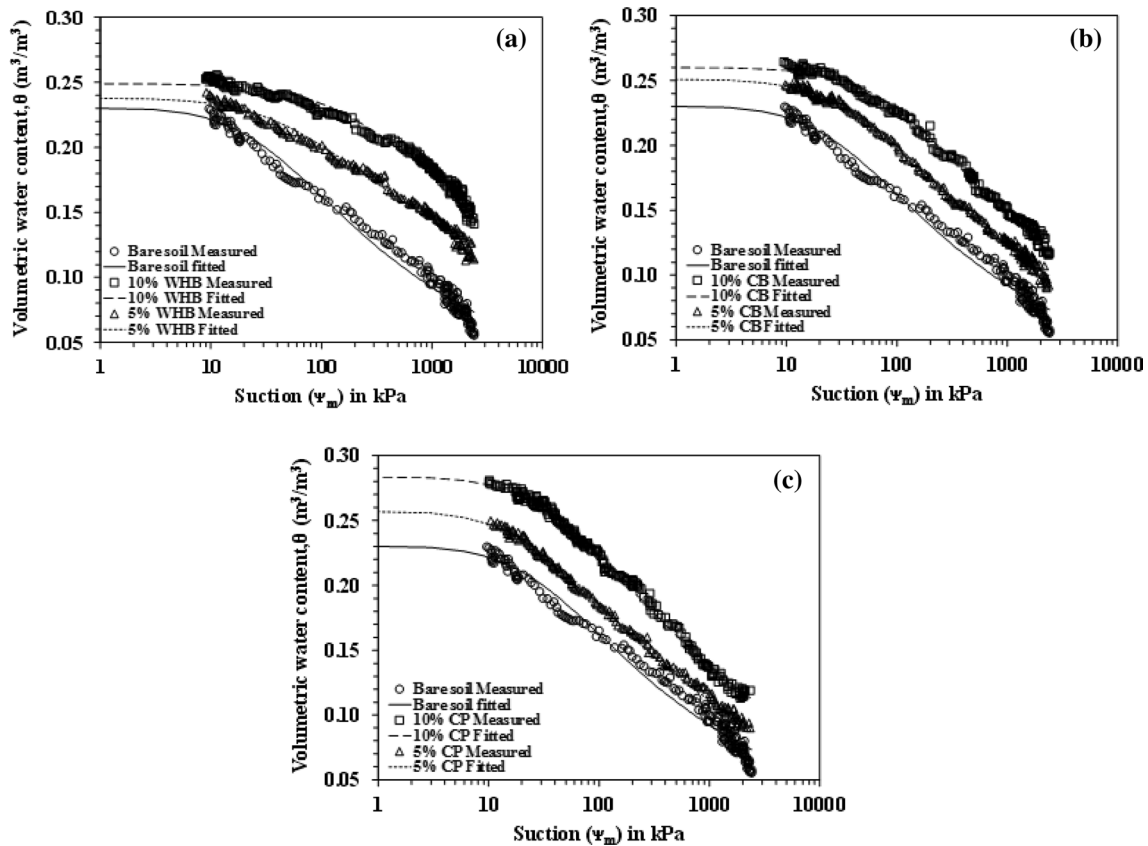

Fig. 6 SWRCs of **a** WHB-amended soil, **b** CB-amended soil and **c** CP-amended soil

Table 3 Fitting parameters of SWRCs fitted using van Genuchten (1980) model

Type	Biochar content (%)	θ_s (%)	θ_r (%)	α (kPa^{-1})	AEV (kPa)	n (−)	$m = (1-1/n)$	R^2 value
Bare soil	0	23	0	0.033	29.92	1.261	0.21	0.980
WHB	5	24	0	0.020	48.16	1.164	0.141	0.983
	10	25	0	0.006	169.73	1.174	0.148	0.980
CB	5	25	0	0.019	51.67	1.242	0.195	0.994
	10	26	0	0.009	104.66	1.25	0.200	0.990
CP	5	26	0	0.035	28.4	1.236	0.191	0.994
	10	28.5	0	0.022	46.3	1.234	0.190	0.994

AEV air entry value

and the intra-porosity by intra-pores. Since, an increase in volume was observed only for CP amended soil when water was added. The adsorption of water in the surface of CP by the hydroxyl (OH) groups present in CP formed larger-size inter-pores between the soil and CP similar to that of soil–fiber composites reported in Bordoloi et al. (2017a) and hence increased porosity. However, this increase in θ_s in CP-amended soil may get suppressed at higher confinement or controlled volume condition. Even though the WHB is more hydrophilic due to the presence of more water-absorbing (OH and COOH) surface functional groups compared with the other amendments (only OH) (Fig. 5), the θ_s was observed to be the lowest in WHB-amended soil. This is attributed to the lowest total porosity in WHB-amended soil compared to the CB- and CP-amended soils, which is evident from the theoretical initial total porosity calculated from initial compaction density and specific gravity. The theoretical total porosity after compaction was observed to be the lowest in WHB-amended soil (34–35% for 5–10% biochar amendment) and the highest in CP-amended soil (39–42%) that caused the variation in θ_s. The lowest total porosity in WHB-amended soil could have occurred either by the decrease in inter-pores size with the settlement of smaller size WHB particles (Table 2) in the inter-pores between soil-soil particles or due to the lower intra-porosity of WHB by the presence of less number and smaller size intra-pores in WHB (relative to CB). The smaller size of intra-pores in WHB was evident by the average pore size measured by the BET analysis (Table 2). In the present study, the crushing of biochar (both WHB and CB) to pass through 2 mm sieve lead to the smaller size particles in WHB compared to the CB (Table 2) that possibly caused a higher destruction of intra-pores in WHB and hence less number of intra-pores in WHB. Spokas et al. (2014) showed a decrease in the number of intra-pores in biochar with the crushing of biochar into smaller particles. The lower intra-porosity of WHB was also evident from the lower water absorption capacity of WHB (54.7 ± 0.99%) compared to the CB (205 ± 12.73%).

The air entry value (AEV) of the soil was observed to increase ($p = 0.09 > 0.05$) with an increase in amendment rate of biochar. The bare soil showed AEV of 29.92 kPa, and it increased to 48.16–51.67 kPa in 5% and 169.73 and 104.66 kPa in 10% WHB- and CB-amended soil respectively. Moreover, a change in AEV was also observed for CP-amended soil. The increased AEV in biochar amendment soil could be attributed to the smaller pore size in biochar-amended soil compared to the bare soil. The settlement of smaller soil or biochar particles in the inter-pores and the presence of smaller size intra-pores in biochar possibly caused the formation of smaller size pores in biochar-amended soil (Abel et al. 2013; Andrenelli et al. 2016). In smaller pores, water is held with a higher suction by capillary action and requires a higher pressure (air pressure) for escape compared to the bare soil therefore higher AEV (Fredlund et al. 2012). The negligible or the absence of intra-pores in CP (Fig. 2h) may be responsible for the negligible variation in AEV with respect to the biochar. Among the biochars, WHB at 10% (w/w) showed the highest AEV while at 5% biochar content, it showed no significant difference. This could be due to the smaller pore size in WHB-amended soil compared to the CB-amended soil by the settlement of smaller-size WHB particles (Table 2) in the inter-pores. The increased AEV in biochar-amended soil would allow the biochar-amended soil to remain saturated for a longer duration compared to the bare soil.

The parameter 'n,' i.e., the slope of the SWRC was observed to decrease slightly ($p = 0.1 > 0.05$) in biochar-amended soil when compared with bare soil (Table 3). The bare soil showed n value of 1.261 and it decreased to 1.164, 1.242 and 1.236 in 5% and 1.174, 1.25 and 1.234 in 10% WHB-, CB- and CP-amended soil, respectively. The smaller pore size in biochar-amended soil compared to the bare soil or the decrease in pore size of the soil after biochar amendment caused the decrease in n value. The amendment of biochar in soil could decrease the size of pores in soil-biochar composites by settling smaller size biochar or soil particles in the inter-pores and increasing the numbers of smaller size intra-pores which is resulting in increased total porosity but decreased pore size compared to the bare soil (Andrenelli et al. 2016). The parameter 'n' represents the desaturation

rate under drying and re-saturation rate under wetting of soil; thus, the decreased 'n' value due to biochar amendment in the present study indicates a slow de-saturation of the soil after AEV.

The residual water content (θ_r) was observed 0 (from the fitting) for all bare and amended soil (Table 3). However, these were not the actual representative of θ_r. The actual θ_r corresponds to a very high suction which has not been reached in the present study under the specified boundary condition and is difficult to measure due to the limitation in most of the measuring instrument. The peak or maximum suction measured in the present study was in the range of 2000–2200 kPa (Fig. 6), and the minimum measured water content ranges from 5.5% in bare soil to 14% in 10% (w/w) WHB-amended soil. Therefore, the effect of biochar on θ_r could not be explained in the present study. In general, the maximum drought stress is considered as wilting point (represented by suction) beyond which plant could not uptake water. A suction of 1500 kPa is often considered as wilting point for most of the plant species (Feddes et al. 1978). Plants or vegetation have immense significance in bioengineered structures due to their capability in providing additional stability (Garg et al. 2015). Hence, instead of θ_r, the water content that corresponds to the suction of 1500 kPa is considered only for comparison, i.e., to see the effect of biochar on water retention at higher suction. The water content at 1500 kPa, i.e., θ_{1500} was observed to increase from 8.3% in bare soil to 16.9% in 10% (w/w) WHB-amended soil. Moreover, among the amendments, WHB-amended soil exhibited the highest increment by 62.65–104% in 5–10% biochar content, whereas CP-amended soil showed the lowest increment by 21% and 50% in 5% and 10% CP content. This increase in θ_{1500} in biochar-amended soil was attributed to the intra-pores along with the functional groups present in biochar that have retained water at higher suction due to their smaller size (nanoscale). The smaller size pores held water tightly due to capillary action that minimizes the water evaporation, and hence, higher water retention. However, the negligible content of intra-pores in CP leads to the lowest increment in θ_{1500}. Further, the presence of smaller intra-pores (Table 2) and the smaller size inter-pores due to embedded fine biochar particles in WHB-amended soil led to the highest increment in θ_{1500}. Thus, smaller pores may be intra-pores or inter-pores retaining water at large suction.

Overall, the increased water retention in the biochar-amended soil is mainly governed by the intra-pores and the inter-pores as hypothesized in Fig. 1. Moreover, the presence of water-absorbing surface functional groups or bond in biochar holds the water inside of these pores especially in intra-pores, i.e., the pores provide only spaces for storage and the functional group holds water in it. The trend of increased water retention in biochar-amended soil was reported by the previous researchers (Bordoloi et al. 2018b; Ni et al. 2018).

However, in previous studies, the effect of different biochars or feedstock type was not considered. In addition, in some studies, the effect of biochar on the different domains of water retention characteristics was not demonstrated, rather simply mentioned increased water retention. The increased water retention in biochar-amended soil that has been characterized by some fitting parameters could be beneficial for the growth of vegetation by reducing irrigation demand and the effect of drought stress as well as less maintenance in bioengineered structures. The higher growth of vegetation due to improved water retention would increase or provide additional stability to the structures against erosion and failure by enhancing the root reinforcement or anchorage, evapotranspiration (suction) and surface coverage.

3.3 Effect of biochar on infiltration

The variation of infiltration rate with suction for bare soil and soil amended with 5–10% (w/w) WHB, CB and CP are depicted in Fig. 7. The infiltration rate obtained at different suction for bare and other amended soils is fitted with an exponential equation, showing the highest R^2 value of 0.8 for bare soil and 0.64–0.73 for other amended soil. It is clear from Fig. 6 that the infiltration rate of the bare soil and all other amended soil decreased with the progressive increase in suction. Moreover, the rate of decrement was observed to be different (being lowest in CP amended soil) among the bare and all other amended soil. Although the infiltration rate of soil naturally increases with suction due to higher water affinity or adsorption tendency at higher suction, the infiltration rate was observed to be decreased. This could be due to the blockage of pores by the entrapped air at higher suction that resists the flow of water into the pores, thereby reducing the infiltration rate (Fredlund et al. 2012).

A decreased infiltration rate compared to the bare soil was observed with an increased biochar amendment rate.
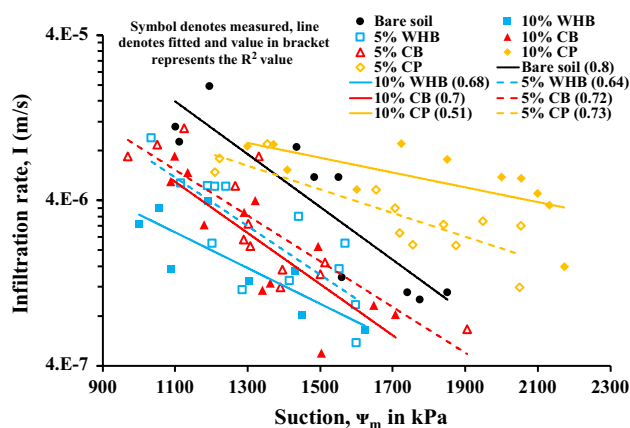
Fig. 7 Variation of infiltration rate with suction for different biochar-amended soils

However, the infiltration rate was observed to be increased with increase in amendment rate of CP. The decreased infiltration rate in biochar-amended soil was attributed to the decrease in inter-pore size compared to the bare soil or the blockage of inter-pores by the settlement of smaller biochar or soil particles. The WHB highly consists of fine particles compared to the bare soil that have a tendency to settle inside the inter-pores between soil-soil particles. The CB consists mostly of larger size particles that the smaller soil particles have the tendency to settle inside the inter-pores between biochar-soil or biochar-biochar particles. The settlement of smaller particles in inter-pores makes the flow path tortuous and hence lower infiltration rate. Moreover, in literature (Ibrahim et al. 2013; Githinji 2014), the hydrophobic nature of some biochar was reported to be responsible for the decrease in infiltration rate. However, in the present study, the biochar (both WHB and CB) was found to be hydrophilic, being higher of WHB (the lowest contact angle) with a contact angle of wetting $< 90°$. The relatively higher hydrophilicity of WHB over the CB was due to the variation in surface functional groups with feedstock type as seen from the FTIR spectra presented in Fig. 5. Thus, the concept of biochar hydrophobicity has no relation to the infiltration rate observed in the present study. Further, the increased infiltration rate in CP-amended soil compared to the bare soil was attributed to the preferential flow occurred through the interface between CP particles or coir fiber and soil particles, similar to the case reported for soil-fiber composite in Bordoloi et al. (2017b). A considerable content of coir fiber in CP could be observed from Fig. 2d. The wetting or saturation of CP-amended soil led to an absorption of water in the surface of coir fiber by the hydroxyl (OH^-) or other oxygen-containing groups present in it, thereby pushing the soil matrix. On further drying, the absorbed water escapes leading to the formation of the preferential path or pore spaces between the interface of soil and fiber (Bordoloi et al. 2017a).

Among the biochars, WHB-amended soil showed lower infiltration rate compared to the CB-amended soil. This could be attributed to the higher content of smaller particles (fines) in WHB (70%) compared to the CB (10%) as mentioned in Table 2 that have decreased or blocked the inter-pores to a higher extent in WHB-amended soil. The higher blocking of pores hinders the water flow path to higher extent leading to the lower infiltration rate. In the existing literature (Ibrahim et al. 2013; Novak et al. 2016), mostly a decreasing trend of infiltration rate in biochar-amended soil compared to the bare soil was documented. Moreover, literature also reported an unchanged infiltration rate of soil after biochar amendment (Busscher et al. 2010; Rogovska et al. 2014). Therefore, the observed decreased infiltration rate in biochar-amended soil in the present study is acceptable and beneficial over unpyrolyzed CP or coir fiber-amended

soil (increased infiltration), in terms of reducing pore water pressure and water percolation in bioengineered structures such as slopes and landfill cover.

3.4 Effect of biochar on desiccation crack

Figure 8 presents the variation of crack intensity factor (CIF) with time for bare soil and soil amended with 5–10% biochar and CP, respectively. In the figure, the zero magnitudes of time represent the day of wetting for saturation of the bare and amended soil samples. The CIF was observed zero for bare and all other amended soil on day zero which is an indication of the saturated condition of the samples. Moreover, the zero CIF was observed to extend up to day 4 after saturation in all amended soil, indicating a prolonged saturation of amended soil compared to the bare soil. It is also supported by the higher AEV in all amended soil compared to the bare soil (Table 3). The CIF was observed further to increase in bare and all amended soil with the increase in duration of the drying after saturation. However, it became constant after reaching a peak value of (2.2 ± 0.1) for bare soil and $(0.78 \pm 0.07$ to $1.47 \pm 0.08)$ for amended soil. The maximum CIF was observed (2.2 ± 0.1) in bare soil, and this could be the maximum crack potential of the soil under the specified compaction density and boundary condition. In a previous study on silty clay compacted at 0.9MDD, Bordoloi et al. (2018a) reported a maximum CIF of (2.65 ± 0.56). However, in the present study soil consist of lower fine (< 0.075 mm) content (49%) against higher content (75%) in Bordoloi et al. (2018a). Therefore, a lower CIF was expectable as soil with lower fine content exhibits lesser cracks compared to soil with higher fine content (Yesiller et al. 2000). The increase in CIF with time was attributed to the decreased soil strength due to drying after wetting, and increased tensile stress developed in soil surface. The shrinkage of soil
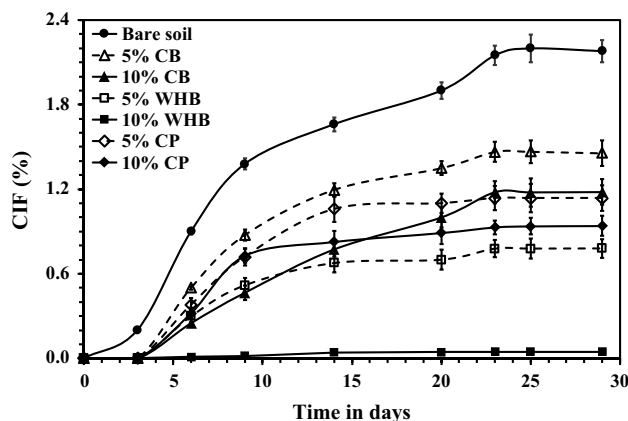

Fig. 8 Variation of surface desiccation crack with time during the drying period for different biochar-amended soils. (Error bar represents the standard error defined by standard deviation)

due to drying causes breaking of microbonds and rearrangement of soil structure, leading to decreased soil strength. Further, the drying or evaporation of water with time causes the generation of higher suction and that in turn led to the development of large tensile stress in the soil surface (Tang et al. 2010). However, the tensile stress developed due to increased suction was maximum at peak CIF, and thereafter, further increase in suction caused no change in tensile stress and hence the CIF (Yesiller et al. 2000).

The CIF was observed to decrease ($p = 0.009 < 0.05$) with an increase in the amendment rate (WHB, CB and CP) from 0% in bare soil to 5–10% (w/w) (Fig. 8). This is attributed to the increased water retention of the soil with the higher amendment rate (Fig. 6). The increased water retention or the higher water content in soil with amendment led to the generation of lower suction or the development of lower tensile stress by a lower loss of water in drying or evaporation compared to the bare soil and hence lower cracks or CIF (Tang et al. 2010). The smaller-size intra-pores in biochar that are responsible for increased water retention in biochar-amended soil hold water tightly and not allow water to escape easily, i.e., reduces water evaporation and hence resist cracks. Among all the amendment (WHB, CB and CP), the WHB-amended soil showed the lowest ($p = 0.15 > 0.05$) CIF, and it was followed by the CP- and CB-amended soil. The lowest CIF in WHB-amended soil is attributed to the highest water retention (the lowest value of 'n' in Table 3) after AEV in WHB-amended soil. Cracks generally start developing after AEV and extend with further increase in suction (Bordoloi et al. 2018b). However, in the WHB-amended soil, the highest water retention after AEV reduced the extending potential of the cracks, leading to the lowest CIF. A trend of decreased CIF or cracking tendency due to the amendment of biochar was also reported in the literature (Zong et al. 2014; Bordoloi et al. 2018b). However, the reported literature has not considered the effect of different biochars or feedstock types that controls the biochar properties. Therefore, the amendment of WHB would be beneficial over the CB and un-pyrolyzed CP in terms of reducing the crack potential. The reduced tendency of crack due to biochar amendment would be beneficial for bioengineered structures, in terms of controlling infiltration rate, excess pore water pressure and maintaining structural stability. Different biochars produced at variable pyrolysis temperature with dissimilar particles size could impose different effect after amending to soil. The different pyrolysis temperatures cause variation in biochar intra-porosity by changing the number and size of intra-pores (Ahmad et al. 2014). The dissimilar particle size could lead to the variable inter-porosity by changing inter-pores size (Lim et al. 2017). The difference in porosity (inter-pores and intra-pores) due to variable pyrolysis temperature and biochar particles size would definitely alter the soil water retention and infiltration

rate that in turn desiccate crack potential. However, in the present study, the pyrolysis condition (pyrolysis temperature and residence time) and particles size were maintained same. Therefore, there should not be any effect of pyrolysis process and biochar particles size expected and ignored.

4 Conclusions

The present study aims to explore the effect of two different biochars on the water retention, infiltration and desiccation crack potential of compacted silty sand. The following conclusions can be drawn:

(1) The water retention is observed to be higher in biochar-amended soil compared to the bare soil. Intra-pores present in biochar are responsible for the altered water retention.

(2) The infiltration rate and the desiccation crack potential of the soil are observed to be decreased after biochar amendment. The alteration in pore size distribution of the soil after biochar amendment contributed to the change.

(3) The amendment of WHB is found to be more effective over the CB in terms of higher water retention at large suction (=> 1500 kPa), lower infiltration rate and desiccation crack potential.

(4) Moreover, the amendment of biochar is found to be advantageous over the un-pyrolyzed coir pith, in terms of higher water retention, lower infiltration rate and desiccation crack potential.

The higher water retention in biochar-amended soil would help in the growth of vegetation in the bioengineered structure in the arid or semiarid region by reducing the effect of drought stress and the demand for irrigation. Similarly, the lower infiltration rate and desiccation crack potential of biochar-amended soil would resist or prevent the development of excess pore water pressure and the percolation of water in bioengineered structures, especially in landfill cover. Future systematic studies are needed to consider the effect of biochar particle size and pyrolysis temperature on soil engineering properties. Further, field-scale studies on the water retention, infiltration and desiccation crack potential of biochar-amended soil are needed to be done for potential application of biochar-amended soil in the real field.

References

Abel S, Peters A, Trinks S, Schonsky H, Facklam M, Wessolek G (2013) Impact of biochar and hydrochar addition on water retention and water repellency of sandy soil. Geoderma 202:183–191

Ahmad M, Rajapaksha AU, Lim JE, Zhang M, Bolan N, Mohan D, Ok YS (2014) Biochar as a sorbent for contaminant management in soil and water: a review. Chemosphere 99:19–33

Albright WH, Benson CH, Gee GW, Abichou T, McDonald EV, Tyler SW, Rock SA (2006) Field performance of a compacted clay landfill final cover at a humid site. J Geotech Geoenviron 132(11):1393–1403

Andrenelli MC, Maienza A, Genesio L, Miglietta F, Pellegrini S, Vaccari FP, Vignozzi N (2016) Field application of pelletized biochar: Short term effect on the hydrological properties of a silty clay loam soil. Agr Water Manage 163:190–196

Angalaeeswari K, Kamaludeen SPB (2017) Production and characterization of coconut shell and mesquite wood biochar. Int J Chem Stud 5:442–446

ASTM C128–15. (2015) Standard test method for relative density (specific gravity) and absorption of fine aggregate. ASTM International, West Conshohocken, PA

ASTM D2487–11. (2011) Standard practice for classification of soils for engineering purpose (unified soil classification system). ASTM International, West Conshohocken, PA

ASTM D422–63 (2007) Standard test method for particle-size analysis of soils. ASTM Int West Conshohocken 10:1520

ASTM D4318–10 (2010) Standard test methods for liquid limit, plastic limit and plasticity index of soils. ASTM International, West Conshohocken, PA

ASTM D4972. (2018) Standard test method for pH of soils. West Conshohocken, PA

ASTM D698–12 (2012) Standard test methods for laboratory compaction characteristics of soil using standard effort. ASTM International, West Conshohocken, PA

ASTM D854 (2010) Standard test method for specific gravity of soil solids by water pycnometer. ASTM International, West Conshohocken, PA

ASTM E1755–01 (2007) Standard method for the determination of ash in biomass 2003 annual book of ASTM standards 11 05. ASTM International, Philadelphia, PA

Bird M, Keitel C, Meredith W (2017) Analysis of biochars for C, H, N, O and S by elemental analyser. In: Biochar: a guide to analytical methods. CSIRO publishing, Clayton, Australia, pp 39

Bordoloi S, Garg A, Sekharan S (2017a) A review of physio-biochemical properties of natural fibers and their application in soil reinforcement. Adv Civil Eng Mater 6(1):323–359

Bordoloi S, Hussain R, Garg A, Sreedeep S, Zhou WH (2017b) Infiltration characteristics of natural fiber reinforced soil. Transp Geotech 12:37–44

Bordoloi S, Hussain R, Gadi VK, Bora H, Sahoo L, Karangat R, Sreedeep S (2018a) Monitoring soil cracking and plant parameters for a mixed grass species. Géotech Lett 8(1):49–55

Bordoloi S, Garg A, Sreedeep S, Lin P, Mei G (2018b) Investigation of cracking and water availability of soil-biochar composite synthesized from invasive weed water hyacinth. Bioresour Technol 263:655–677

Busscher W, Novak J, Evans D, Watts D, Niandou M, Ahmedna M (2010) Influence of pecan biochar on physical properties of a Norfolk loamy sand. Soil Sci 175(1):10–14

Cao CT, Farrell C, Kristiansen PE, Rayner JP (2014) Biochar makes green roof substrates lighter and improves water supply to plants. Ecol Eng 71:368–374

Chen XW, Wong JTF, Ng CWW, Wong MH (2016) Feasibility of biochar application on a landfill final cover—a review on balancing ecology and shallow slope stability. Environ Sci Pollut R 23(8):7111–7125

Chen W, Meng J, Han X, Lan Y, Zhang W (2019) Past, present, and future of biochar. Biochar 1(1):75–87

Coles N, Trudgill S (1985) The movement of nitrate fertiliser from the soil surface to drainage waters by preferential flow in weakly structured soils, Slapton. S Devon Agr Ecosyst Environ 13(3–4):241–259

Corte A, Higashi A (1964) Experimental research on desiccation cracks in soil (No. RR-66). Cold Regions Research and Engineering Lab, Hanover, NH, USA

Costa S, Kodikara J, Shannon B (2013) Salient factors controlling desiccation cracking of clay in laboratory experiments. Géotechnique 63(1):18

de Melo Carvalho MT, Maia ADHN, Madari BE, Bastiaans L, Van Oort PAJ, Heinemann AB, Meinke H (2014) Biochar increases plant available water in a sandy soil under an aerobic rice cropping system. Solid Earth 6:887–917

Decagon Devices (2016) Operator's manual version 2. MPS-2 & MPS-6 Dielectric Water Potential Sensors. Decagon Devices Inc., NE Nelson Court, Pullman, WA 99163, USA

Downie A, Crosky A, Munroe P (2009) Physical properties of biochar. Biochar for environmental management: Science Technology. Routledge, London, UK, pp 13–32

Feddes RA, Kowalik PJ, Zaradny H (1978) Simulation of field water use and crop yield. Centre for Agricultural Publishing and Documentation, Wageningen, Netherlands

Fellet G, Marchiol L, Delle Vedove G, Peressotti A (2011) Application of biochar on mine tailings: effects and perspectives for land reclamation. Chemosphere 83(9):1262–1267

Fodor N, Sándor R, Orfanus T, Lichner L, Rajkai K (2011) Evaluation method dependency of measured saturated hydraulic conductivity. Geoderma 165(1):60–68

Fredlund DG, Rahardjo H, Fredlund MD (2012) Unsaturated soil mechanics in engineering practice. Wiley, Hoboken

Gadi VK, Bordoloi S, Garg A, Sahoo L, Berretta C, Sekharan S (2017) Effect of shoot parameters on cracking in vegetated soil. Environ Geotech 5(2):1–31

Garg A, Leung AK, Ng CWW (2015) Transpiration reduction and root distribution functions for a non-crop species Schefflera heptaphylla. CATENA 135:78–82

Githinji L (2014) Effect of biochar application rate on soil physical and hydraulic properties of a sandy loam. Arch Agron Soil Sci 60(4):457–470

Goldsmith W, Silva M, Fischenich C (2001) Determining optimal degree of soil compaction for balancing mechanical stability and plant growth capacity (No. ERDC-TN-EMRRP-SR-26). Engineer research and development center. Vicksburg, MS environmental lab

Harshani HMD, Nawagamuwa UP, Senanayake A (2015) Evaluation of cover soil properties of solid waste dumpsites in Colombo district, Sri Lanka. J Nat Sci Found Sri Lanka 43:2

Hussain R, Garg A, Ravi K (2020a) Soil-biochar-plant interaction: differences from the perspective of engineered and agricultural soils. Bull Eng Geol Environ. https://doi.org/10.1007/s10064-020-01846-3

Hussain R, Ravi K, Garg A (2020) Influence of biochar on the soil water retention characteristics (SWRC): Potential application in geotechnical engineering structures. Soil Tillage Res 204:104713

Ibrahim HM, Al-Wabel MI, Usman AR, Al-Omran A (2013) Effect of Conocarpus biochar application on the hydraulic properties of a sandy loam soil. Soil Sci 178(4):165–173

Igalavithana AD, Ok YS, Niazi NK, Rizwan M, Al-Wabel MI, Usman AR, Lee SS (2017) Effect of corn residue biochar on the hydraulic properties of sandy loam soil. Sustainability 9(2):266

Indraratna B, Muttuvel T, Khabbaz H, Armstrong R (2008) Predicting the erosion rate of chemically treated soil using a process simulation apparatus for internal crack erosion. J Geotech Geoenviron Eng 134(6):837–844

Jeffery S, Meinders MB, Stoof CR, Bezemer TM, van de Voorde TF, Mommer L, van Groenigen JW (2015) Biochar application does

not improve the soil hydrological function of a sandy soil. Geoderma 251:47–54

Lehmann J, Joseph S (2015) Biochar for environmental management: science, technology and implementation. Routledge, New York, USA

Lei O, Zhang R (2013) Effects of biochars derived from different feedstocks and pyrolysis temperatures on soil physical and hydraulic properties. J Soil Sediment 13(9):1561–1572

Li JH, Li L, Chen R, Li DQ (2016) Cracking and vertical preferential flow through landfill clay liners. Eng Geol 206:33–41

Lim TJ, Spokas KA, Feyereisen GW, Weis R, Koskinen WC (2017) Influence of biochar particle size and shape on soil hydraulic properties. J Environ Sci Eng 5(1):8–15

Major J, Rondon M, Molina D, Riha SJ, Lehmann J (2012) Nutrient leaching in a Colombian savanna Oxisol amended with biochar. J Environ Qual 41(4):1076–1086

Malik A (2007) Environmental challenge vis a vis opportunity: the case of water hyacinth. Environ Int 33(1):122–138

Moragues-Saitua L, Arias-González A, Gartzia-Bengoetxea N (2017) Effects of biochar and wood ash on soil hydraulic properties: a field experiment involving contrasting temperate soils. Geoderma 305:144–152

Ni J, Chen X, Ng C, Guo H (2018) Efects of biochar on water retention and matric suction of vegetated soil. Géotechnique Lett 8(2):124–129

Novak J, Sigua G, Watts D, Cantrell K, Shumaker P, Szogi A, Spokas K (2016) Biochars impact on water infiltration and water quality through a compacted subsoil layer. Chemosphere 142:160–167

Ouyang L, Wang F, Tang J, Yu L, Zhang R (2013) Effects of biochar amendment on soil aggregates and hydraulic properties. J Soil Sci Plant Nut 13(4):991–1002

Prober SM, Stol J, Piper M, Gupta VVSR, Cunningham SA (2014) Enhancing soil biophysical condition for climate-resilient restoration in mesic woodlands. Ecol Eng 71:246–255

Rasband WS (2011) ImageJ US National Institutes of Health, Bethesda, 616 Maryland, Astrophysics Source Code Library, USA

Reddy KR, Yargicoglu EN, Yue D, Yaghoubi P (2014) Enhanced microbial methane oxidation in landfill cover soil amended with biochar. J Geotech Geoenviron 140(9):04014047

Reddy KR, Yaghoubi P, Yukselen-Aksoy Y (2015) Effects of biochar amendment on geotechnical properties of landfill cover soil. Waste Manage Res 33(6):524–532

Rogovska N, Laird DA, Rathke SJ, Karlen DL (2014) Biochar impact on Midwestern Mollisols and maize nutrient availability. Geoderma 230:340–347

Spokas KA, Novak JM, Masiello CA, Johnson MG, Colosky EC, Ippolito JA, Trigo C (2014) Physical disintegration of biochar: an overlooked process. Environ Sci Tech Let 1(8):326–332

Suliman W, Harsh JB, Abu-Lail NI, Fortuna AM, Dallmeyer I, Garcia-Pérez M (2017) The role of biochar porosity and surface functionality in augmenting hydrologic properties of a sandy soil. Sci Total Environ 574:139–147

Tan X, Liu Y, Zeng G, Wang X, Hu X, Gu Y, Yang Z (2015) Application of biochar for the removal of pollutants from aqueous solutions. Chemosphere 125:70–85

Tang CS, Shi B, Liu C, Gao L, Inyang HI (2010) Experimental investigation of the desiccation cracking behavior of soil layers during drying. J Mater Civil Eng 23(6):873–878

Thomas GW (1982) Exchangeable cations. Methods of soil analysis. Part 2. Chemical and microbiological properties, (methodsofsoilan2). Amer Soc of Agron Inc.: Madison, Wisconsin, USA, pp 159–165

Uzoma KC, Inoue M, Andry H, Zahoor A, Nishihara E (2011) Influence of biochar application on sandy soil hydraulic properties and nutrient retention. J Food Agric Environ 9(3–4):1137–1143

van Genuchten M (1980) A closed-form equation for predicting the hydraulic conductivity of unsaturated soils. Soil Sci Soc Am J 44(5):892–898

van Genuchten MV, Leij FJ, Yates SR (1991) The RETC code for quantifying the hydraulic functions of unsaturated soils. USEPA, Washington, DC

Van Zwieten L, Kimber S, Morris S, Chan KY, Downie A, Rust J, Cowie A (2010) Effects of biochar from slow pyrolysis of paper-mill waste on agronomic performance and soil fertility. Plant Soil 327(1–2):235–246

Wall DK, Zeiss C (1995) Municipal landfill biodegradation and settlement. J Environ Eng 121(3):214–224

Williams JM, Latifi N, Vahedifard F (2018) In: Effects of biochar amendment on mechanical properties of buckshot clay. IFCEE, Orlando, Florida, pp 125–134

Wong JTF, Chen Z, Ng CWW, Wong MH (2016) Gas permeability of biochar-amended clay: potential alternative landfill final cover material. Environ Sci Pollut R 23(8):7126–7131

Wong JTF, Chen Z, Chen X, Ng CWW, Wong MH (2017) Soil-water retention behavior of compacted biochar-amended clay: a novel landfill final cover material. J Soil Sediment 17(3):590–598

Wong JTF, Chen Z, Wong AYY, Ng CWW, Wong MH (2018) Effects of biochar on hydraulic conductivity of compacted kaolin clay. Environ Pollut 234:468–472

Wu TH, McKinnell WP III, Swanston DN (1979) Strength of tree roots and landslides on Prince of Wales Island. Alaska Can Geot J 16(1):19–33

Wu P, Ata-Ul-Karim ST, Singh BP, Wang H, Wu T, Liu C, Chen W (2019) A scientometric review of biochar research in the past 20 years (1998–2018). Biochar 1(1):23–43

Yaghoubi P, Reddy KR (2011) Characteristics of biochar-amended soil cover for landfill gas mitigation. In Pan-Am CGS Geotechnical Conference

Yang X, Meng J, Lan Y, Chen W, Yang T, Yuan J, Han J (2017) Effects of maize stover and its biochar on soil CO2 emissions and labile organic carbon fractions in Northeast China. Agric Ecosyst Environ 240:24–31

Yargicoglu EN, Reddy KR (2017) Biochar-amended soil cover for microbial methane oxidation: effect of biochar amendment ratio and cover profile. J Geotech Geoenviron Eng 144(3):04017123

Yesiller N, Miller CJ, Inci G, Yaldo K (2000) Desiccation and cracking behavior of three compacted landfill liner soils. Eng Geol 57(1):105–121

Zong Y, Chen D, Lu S (2014) Impact of biochars on swell–shrinkage behavior, mechanical strength, and surface cracking of clayey soil. J Plant Nutr Soil Sc 177(6):920–926